An Improved Model-based Polarimetric Decomposition Preserving Dominant Scattering Characteristics

Yongjun Cai[1,2], **Xiangkun Zhang**[2], **and Jingshan Jiang**[2]

[1]University of Chinese Academy of Sciences, China

[2]CAS Key Laboratory of Microwave Remote Sensing, National Space Science Center, CAS, China

Abstract— Original three-component polarimetric decomposition always suffers from some deficiencies such as negative power and scattering mechanism ambiguity. In fact, it is probably because of the inconsistency between the assumed models and PolSAR data. In this paper, we intend to solve the scattering mechanism ambiguity in original three-component decomposition, and later we will try to find out some solutions aiming at alleviating the negative power problem. Considering that the nonnegative eigenvalue decomposition (NNED) is only applicative for the pixels that volume scattering dominates (the details will be discussed in Section 1), an improved model-based scheme is proposed, in which the decomposition will be hierarchical. If volume scattering is dominant, a revised NNED is adopted, for which the volume scattering employs the model proposed by Yamaguchi, and if volume scattering is not dominant, a revised four-component decomposition is adopted, for which the volume scattering employs the model proposed by Freeman. The entropy and alpha parameter are employed to identify the dominant scattering mechanism. Through this revision, the decomposition will be more accurate and the dominant scattering mechanism in each pixel will be preserved better. To verify and demonstrate the performance and advantages of the proposed decomposition, the L-band airborne AIRSAR San Francisco data and E-SAR Oberpfaffenhofen polarimetric data are used. Comparison studies are also carried out to show the improvements by the proposed method especially for the oriented urban areas.

1. INTRODUCTION

In the original model-based three-component decomposition, the volume scattering is subtracted from the original data prior to surface or dihedral scattering, which not surprisingly results in the overestimation of volume scattering power as well as negative power in remainder scattering mechanisms. Owing to the overestimation of volume scattering power, research on model-based polarimetric decomposition has reached a climax in recent several years. The representatives are Yamaguchi decomposition with orientation angle compensation and NNED. However, deorientation cannot solve these problems fundamentally, because the double bounce or surface scattering objects will not always be rotated to the reflection symmetry condition as the original assumed models predict. So in order to extract the scattering objects better, we should develop and adopt more suitable and adaptive models. Details will be discussed in Section 2. NNED is a wonderful way to avoid negative powers completely. But it is under the assumption that the residual matrix has the rank of two, which cannot be applied to the strongly depolarized situation expect the volume scattering. In fact this defaults to the dominance of volume scattering. So in this paper, this will be used for the pixels that volume scattering dominates.

2. GENERALIZED SCATTERING MODELS

For model-based polarimetric decomposition techniques, we think we should firstly start from the models themselves. So we should develop more suitable models for the PolSAR data. In this paper, we consider a generalized scattering model for surface or double bounce scattering, which takes the condition that the oriented surface or dihedral objects can also contribute significant cross-polarization component. Details will be discussed below.

Assuming the measured coherency matrix to be,

$$[T] = \begin{pmatrix} T_{11} & T_{12} & T_{13} \\ T_{21} & T_{22} & T_{23} \\ T_{31} & T_{32} & T_{33} \end{pmatrix} \tag{1}$$

the coherency matrix after rotation by angel θ can be obtained by,

$$R_\theta = \begin{pmatrix} 1 & 0 & 0 \\ 0 & \cos 2\theta & \sin 2\theta \\ 0 & -\sin 2\theta & \cos 2\theta \end{pmatrix}, \quad [T(\theta)] = R_\theta [T] R_\theta^{-1} \tag{2}$$

2.1. Surface Scattering Model

The surface scattering component consists of a first-order Bragg scatterer in which the cross-polarization component is negligible. The scattering matrix has the form,

$$S = \begin{bmatrix} R_H & 0 \\ 0 & R_V \end{bmatrix} \tag{3}$$

in Freeman decomposition and Yamaguchi decomposition, the coherency matrix of surface scattering model is represented as follows,

$$[T_s] = \begin{pmatrix} 1 & \beta^* & 0 \\ \beta & |\beta|^2 & 0 \\ 0 & 0 & 0 \end{pmatrix} \tag{4}$$

where $\beta = (R_H - R_V)/(R_H + R_V)$, $|\beta| < 1$, β is unknown to be determined.

Because terrain slopes could rotate the polarization basis and induce significant cross-polarization component. In order to fit the actual environment, a generalized model for it should be adopted. According to (2), the generalized surface scattering model can be obtained by the multiplication of a unitary rotation matrix $R(\theta)$ as seen in (2),

$$[T_s(\theta)] = R(\theta) \begin{pmatrix} 1 & \beta^* & 0 \\ \beta & |\beta|^2 & 0 \\ 0 & 0 & 0 \end{pmatrix} R(\theta)^{-1} = \begin{pmatrix} 1 & \beta^* \cos 2\theta & -\beta^* \sin 2\theta \\ \beta \cos 2\theta & |\beta|^2 \cos^2 2\theta & -|\beta|^2 \sin 2\theta \cos 2\theta \\ -\beta \sin 2\theta & -|\beta|^2 \sin 2\theta \cos 2\theta & |\beta|^2 \sin^2 2\theta \end{pmatrix} \tag{5}$$

2.2. Double Bounce Scattering Model

The double bounce scattering component consists of a dihedral corner reflector, such as the reflection between the building block walls and the underlying surfaces such as roads. The scattering matrix can be written as follows,

$$S = \begin{bmatrix} e^{j2\gamma_H} R_H & 0 \\ 0 & e^{j2\gamma_V} R_V \end{bmatrix} \tag{6}$$

in Freeman decomposition and Yamaguchi decomposition, the coherency matrix is represented as follows,

$$[T_d] = \begin{pmatrix} |\alpha|^2 & \alpha & 0 \\ \alpha^* & 1 & 0 \\ 0 & 0 & 0 \end{pmatrix} \tag{7}$$

where $\alpha = (R_H + e^{j\phi} R_V)/(R_H - e^{j\phi} R_V)$, $|\alpha| < 1$ and $\phi = 2\gamma_V - 2\gamma_H$.

Obviously, this model also doesn't take the possible cross-polarization component induced by the oriented buildings into consideration. Let the induced orientation angel be θ, the double bounce scattering model can be obtained by the same way,

$$[T_d(\theta)] = R(\theta) \begin{pmatrix} |\alpha|^2 & \alpha & 0 \\ \alpha^* & 1 & 0 \\ 0 & 0 & 0 \end{pmatrix} R(\theta)^{-1} = \begin{pmatrix} |\alpha|^2 & \alpha \cos 2\theta & -\alpha \sin 2\theta \\ \alpha^* \cos 2\theta & \cos^2 2\theta & -\sin 2\theta \cos 2\theta \\ -\alpha^* \sin 2\theta & -\sin 2\theta \cos 2\theta & \sin^2 2\theta \end{pmatrix} \tag{8}$$

3. EXTRACTING DOMINANT SCATTERING MECHANISM

The entropy H and alpha parameters are firstly proposed by Cloude and Pottier, which are wonderful parameters to distinguish different scattering mechanisms, and based on which the H/alpha classification scheme was also proposed, the H/alpha space is given as Figure 1 shows.

The dominance of this space is given as follows,

- **Class Z1, 2 and 3**: Double bounce scattering,
- **Class Z4, 5 and 6**: Volume scattering,
- **Class Z7 and 8**: Surface scattering.

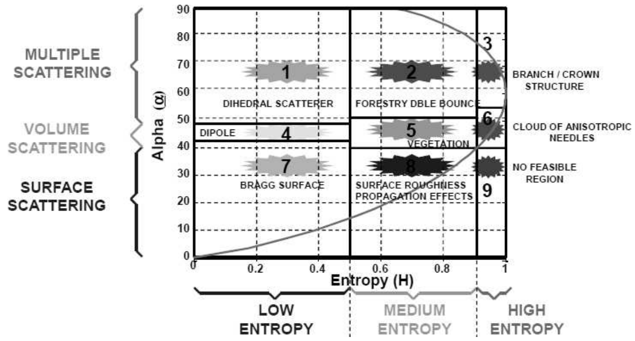

Figure 1: Segmentation of the H/alpha space.

4. DECOMPOSITION FRAMEWORK

The proposed decomposition framework was divided into three individual parts according to the dominant scattering mechanism, so if one pixel belongs to Z7 and 8 in Figure 1, the decomposition will be written as follows,

$$\begin{aligned}\langle[T]\rangle &= f_s\langle[T_s(\theta)]\rangle + f_d\langle[T_d]\rangle + f_v\langle[T_v]\rangle + f_c\langle[T_c]\rangle \\ &= f_s\begin{pmatrix} 1 & \beta^*\cos 2\theta & -\beta^*\sin 2\theta \\ \beta\cos 2\theta & |\beta|^2\cos^2 2\theta & -|\beta|^2\sin 2\theta\cos 2\theta \\ -\beta\sin 2\theta & -|\beta|^2\sin 2\theta\cos 2\theta & |\beta|^2\sin^2 2\theta \end{pmatrix} + f_d\begin{pmatrix} 0 & 0 & 0 \\ 0 & 1 & 0 \\ 0 & 0 & 0 \end{pmatrix} \\ &\quad + \frac{f_v}{4}\begin{pmatrix} 2 & 0 & 0 \\ 0 & 1 & 0 \\ 0 & 0 & 1 \end{pmatrix} + \frac{f_c}{2}\begin{pmatrix} 0 & 0 & 0 \\ 0 & 1 & \pm j \\ 0 & \mp j & 1 \end{pmatrix} \end{aligned} \tag{9}$$

under this circumstance, the surface scattering is dominant, so the surface parameter should be solved explicitly.

While if one pixel belongs to Z1, 2 and 3, the decomposition is written as follows, similarly, the double bounce parameter should be solved explicitly,

$$\begin{aligned}\langle[T]\rangle &= f_d\langle[T_d(\theta)]\rangle + f_s\langle[T_s]\rangle + f_v\langle[T_v]\rangle + f_c\langle[T_c]\rangle \\ &= f_d\begin{pmatrix} |\alpha|^2 & \alpha\cos 2\theta & -\alpha\sin 2\theta \\ \alpha^*\cos 2\theta & \cos^2 2\theta & -\sin 2\theta\cos 2\theta \\ -\alpha^*\sin 2\theta & -\sin 2\theta\cos 2\theta & \sin^2 2\theta \end{pmatrix} + f_s\begin{pmatrix} 1 & 0 & 0 \\ 0 & 0 & 0 \\ 0 & 0 & 0 \end{pmatrix} \\ &\quad + \frac{f_v}{4}\begin{pmatrix} 2 & 0 & 0 \\ 0 & 1 & 0 \\ 0 & 0 & 1 \end{pmatrix} + \frac{f_c}{2}\begin{pmatrix} 0 & 0 & 0 \\ 0 & 1 & \pm j \\ 0 & \mp j & 1 \end{pmatrix} \end{aligned} \tag{10}$$

At last, if one pixel belongs to Z4, 5 and 6, that is the volume scattering dominant, general NNED with the volume scattering model proposed by Yamaguchi will be adopted instead. Because the volume scattering parameter should be solved explicitly.

It should be pointed out that because the unknown parameters we propose are unbalanced with the observations, consequently, the results of Equations (9) and (10) are both not unique. Therefore, for each solution, we then perform it to all pixels and then compare the numbers of negative powers by them, at last, we pick the solution that leaves the smallest relative amount of negative powers as the ultimate result. What's more, the models are scarcely possible to fit the data perfectly, so that the negative powers still inevitably exist in each of the results, so for the pixels with negative power, we use the Yamaguchi scheme instead this time. And later we will try to alleviate negative power problem by fitting data into models.

5. EXPERIMENTS AND RESULTS

The performance of the proposed approach is demonstrated using the AIRSAR San Francisco data sets. Figures 2(a), (b) show the decomposed results by the Yamaguchi scheme and the proposed. Figure 2(c), (d) show the close-ups of Patch B of Figures 2(a), (b), from the close-ups, we can clearly see the change in orientated buildings after the proposed decomposition is carried out. The more

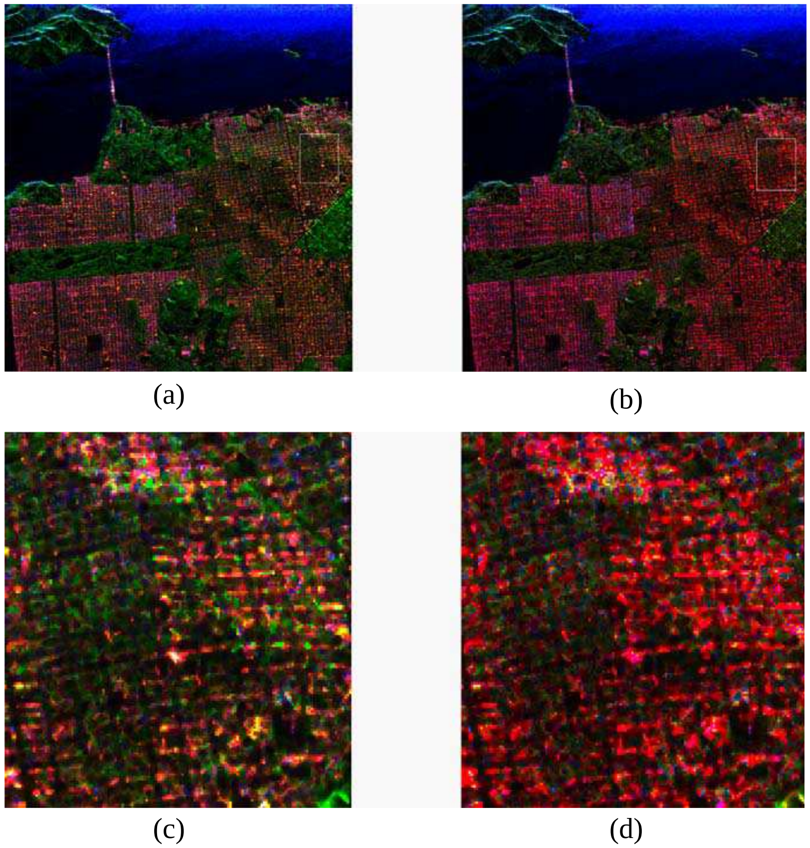

Figure 2: (a) Results of Yamaguchi decomposition and (b) the proposed; (c), (d) close-ups of patches in (a), (b).

pixels in urban areas in Yamaguchi decomposition have been decomposed into red color, which indicates the dihedral scattering mechanism from the building walls and the roads. This means that the buildings correctly turn into red color or to say the red color in urban areas is got enhanced although they are oriented in different directions. It shows that it is possible to discriminate the urban areas from forest areas, i.e., the ambiguity in original Freeman and Yamaguchi decomposition has been alleviated by the proposed decomposition.

REFERENCES

1. Cloude, S. R. and E. Pottier, "A review of target decomposition theorems in radar polarimetry," *IEEE Trans. Geosci. Remote Sens.*, Vol. 34, No. 2, 498–518, 1996.
2. Freeman, A. and S. L. Durden, "A three-component scattering model for polarimetric SAR data," *IEEE Trans. Geosci. Remote Sens.*, Vol. 36, No. 3, 963–973, 1998.
3. Yamaguchi, Y., A. Sato, W. M. Boerner, R. Sato, and H. Yamada, "Four component scattering power decomposition with rotation of coherency matrix," *IEEE Trans. Geosci. Remote Sens.*, Vol. 49, No. 6, 2251–2258, 2011.
4. Van Zyl, J. J., M. Arii, and Y. Kim, "Model-based decomposition of polarimetric SAR covariance matrices constrained for nonnegative eigenvalues," *IEEE Trans. Geosci. Remote Sens.*, Vol. 49, No. 9, 3452–3459, 2011.
5. Cui, Y., Y. Yamaguchi, J. Yang, H. Kobayashi, S. E. Park, and G. Singh, "On complete model-based decomposition of polarimetric SAR coherency matrix data," *IEEE Trans. Geosci. Remote Sens.*, No. 52, No. 4, 1991–2001, 2014.